

RSC Advances



This is an *Accepted Manuscript*, which has been through the Royal Society of Chemistry peer review process and has been accepted for publication.

Accepted Manuscripts are published online shortly after acceptance, before technical editing, formatting and proof reading. Using this free service, authors can make their results available to the community, in citable form, before we publish the edited article. This *Accepted Manuscript* will be replaced by the edited, formatted and paginated article as soon as this is available.

You can find more information about *Accepted Manuscripts* in the [Information for Authors](#).

Please note that technical editing may introduce minor changes to the text and/or graphics, which may alter content. The journal's standard [Terms & Conditions](#) and the [Ethical guidelines](#) still apply. In no event shall the Royal Society of Chemistry be held responsible for any errors or omissions in this *Accepted Manuscript* or any consequences arising from the use of any information it contains.

Effects of LAGP Electrolyte on Suppressing Polysulfides Shuttle in Li-S Cell

Xue-ling Wu,^{ab} Jun Zong,^{ab} Han Xu,^{ab} Wei Wang,^a and Xing-jiang Liu^{*ab}

a) Department of Applied Chemistry, School of Chemical Engineering & Technology, Tianjin

University, Tianjin 300072, P.R. China

b) National Key Lab of Power Sources, Tianjin Institute of Power Sources, Tianjin 300384, P.R. China

* Corresponding author: Tel: +86-2223959300, Fax: +86-2223383783, e-mail address: xjliu@nkplps.org

Abstract: In this work, the solid electrolyte of $\text{Li}_{1.5}\text{Al}_{0.5}\text{Ge}_{1.5}(\text{PO}_4)_3$ (LAGP) is used to suppress polysulfides shuttle in Li-S cell. Firstly, the H-type visible cell is assembled by using the LAGP glass ceramic plate and normal poly-propylene (PP) separator, respectively. It is demonstrated that the LAGP glass ceramic plate is quite effective in shutting-down the migration of polysulfides ions and improving the utilization ratio of sulfur cathode. However, the commercial production of Li-S battery is not possible to use the LAGP glass ceramic plate as a membrane due to its brittle characteristics. Herein, the LAGP modified separator has been prepared by simple casting procedure and applied in Li-S cell. The Li-ion conductivity of the LAGP modified separator is $6.280 \times 10^{-4} \text{ S cm}^{-1}$ at room temperature. The Li-ion transference number and the Gurley value of the modified separator show that the diffusion of the polysulfide anions can be suppressed effectively. The discharge capacity of the Li-S cell with the modified separator at the 50 th cycle can reach $770.1 \text{ mA h g}^{-1}$, while that of the Li-S cell with routine PP separator is only $658.4 \text{ mA h g}^{-1}$ at the 50th cycle. The superior utilization of sulfur in the Li-S cells indicates that using LAGP modified separator is a viable way to overcome the shuttle problem for practical Li-S batteries.

1. Introduction

Li-S battery is a promising prospect for electrochemical energy storage devices due to its high theoretical gravimetric capacity of 1675 mAh g⁻¹ and energy density of 2600 Wh kg⁻¹, low cost, high abundance, and nontoxicity. Therefore, the Li-S battery system is considered as a choice of post-lithium ion era. However, despite great efforts in the past years, the commercial application for Li-S battery has been hindered by several technical issues.¹ One of the biggest bottlenecks is the insulating nature of sulfur and its discharge product Li₂S,² which leads to poor active material utilization and decrease in discharge capacity. Another challenge involves the rapid capacity fading that is attributed to the high solubility of the long-chain polysulfide ions generating during charge/discharge process. The dissolved lithium polysulfides freely diffuse through the separator and then shuttle between the cathode and anode, resulting in low coulombic efficiency and utilization of the active materials.³

To overcome the intractable shuttle effect of Li-S batteries, several approaches have been proposed during the past ten years. A common strategy is used to confine sulfur into porous frameworks, such as porous carbon materials,^{4,5} metal oxide matrix,^{6,7} and polymer matrix.^{8,9} During cycling, the lithium polysulfides are anchored in the cathode by the above materials through physical or chemical adsorption, suppressing polysulfides dissolution in the electrolyte and thus movement to the anode. Another feasible approach is to protect the lithium surface from reaction with polysulfides by applying LiNO₃ additive in the LiTFSI/DOL+DME electrolyte.¹⁰⁻¹² In fact, LiNO₃ is consumed during SEI formation and will decompose in Li-S cells at potential below 1.6 V vs. Li/Li⁺.¹³ In order to further restrain polysulfides from diffusing, the widespread attention has been paid to the physical barrier for polysulfides between the cathode and the separator. From the reported literature, the physical barrier mainly includes the interlayer and the modified separator. Recently, the nano-Li⁺-channel interlayer,¹⁴ mesoporous carbon interlayers,¹⁵ free standing MWCNT paper,¹⁶ self-assembly polypyrrole nanotube film,¹⁷ treated carbon paper,¹⁸ and reduced graphene oxide based film¹⁹ have been used to improve capacity retention of Li-S cells. Moreover, various membrane treatments through coating processes on a separator, such as montmorillonite (MMT) ceramic protective film,²⁰ Al₂O₃-coated porous separator,²¹ Nafion-coated PP separator,²² and bifunctional MCNT@PEG-modified separator²³ have been utilized in Li-S cell to enhance cell cycle performance. However, the carbon materials, polymers, Al₂O₃ as well as MMT ceramic powders are not a lithium-ion conductor.

As for the lithium ion conductors, the crystalline oxide can not fail to mention, which includes

perovskite-type, LISICON-type, garnet-type as well as NASICON-type oxide.²⁴ And solid ionic conductor of $\text{Li}_{1.5}\text{Al}_{0.5}\text{Ge}_{1.5}(\text{PO}_4)_3$ (LAGP) based on a $\text{LiM}_2(\text{PO}_4)_3$ [M = Ti, Ge, *etc.* is a metal] structure is an important member of Li-ion conductive ceramics with the NASION (Na super ion conductor) type structure, which possess several advantages in terms of electrical conductivity, electrochemical window, and stability in ambient atmosphere.²⁵ Recently, to eliminate the shuttle effect of polysulfides, a novel Li-S battery system was developed with a dual-phase electrolyte, in which the LAGP (LATP) electrolyte was used to separate the liquid electrolytes for the cathode and the anode.²⁶⁻³¹ But the LAGP modified separator, not the glass ceramic plate, was scarcely used to suppress polysulfides shuttle in Li-S cell.

In this work, the LAGP modified separator is prepared from the LAGP powders, which was coated on the surface of the routine PP separator. After modifying the PP separator by LAGP, the utilization of sulfur could be increased in Li-S batteries. These results indicate that the LAGP modified separator is suitable to be applied to overcome the shuttle phenomenon of Li-S cell.

2. Experimental

Materials

Lithium carbonate (Li_2CO_3 , 99%), Aluminium oxide (Al_2O_3 , 99.99%) and ammonium dihydrogen phosphate ($\text{NH}_4\text{H}_2\text{PO}_4$, AR) were purchased from Shanghai Aladdin Bio-Chem Technology Co., Ltd. Germanium Oxide (GeO_2 , 99.999%) was purchased from Alfa Aesar (China) Chemical Co., Ltd, China. Sublimed sulfur (S, 99.5%) was purchased from Sigma Aldrich Co., Ltd. Vapor-grown carbon fiber (VGCF) was purchased from SHOWA DENKOK.K Co., Ltd. Ketjen black (KB) was purchased from Triquo Chemical Co., Ltd, China. LA133 binder was purchased from Chengdu Indigo Power Sources Co., Ltd. Polyvinylidene difluoride (PVDF) and N-methyl-2-pyrrolidinone (NMP) were purchased from Shanghai Kureha Chemical Ltd. Super P (SP), Li foil and Celgard 2300 were purchased from Hefei Kejing Material Technology Co., Ltd, China. 1M lithium bis(trifluoromethanesulfonyl)imide (LiTFSI) (dissolved in 1,3-dioxolane (DOL), 1,2-dimethoxyethane (DME) with a volume ratio of 1:1) was purchased from Tianjin Jinniu Power Sources Material Co., Ltd, China. The electrolyte additive of LiNO_3 was purchased from Sigma Aldrich Co., Ltd. All the chemicals were of analytical grade and were used as-received without further purification.

Preparation of nominal composition LAGP

Stoichiometric amount of Li_2CO_3 , Al_2O_3 , GeO_2 and $\text{NH}_4\text{H}_2\text{PO}_4$ (0.75:0.25:1.5:3 in mol%, and an

additional 10 wt% of Li_2CO_3 to compensate for the Li loss during heat treatment) were used as starting materials to prepare $\text{Li}_{1.5}\text{Al}_{0.5}\text{Ge}_{1.5}(\text{PO}_4)_3$ (LAGP) by the solid-state reaction. The powders were uniformly mixed by planetary ball milling and calcined in an alumina crucible at 700 °C for 2 h in the box furnace to form the LAGP phase, then, LAGP powder was ground again and melted at 1350 °C. A clear, homogeneous, and viscous melt was poured onto preheated stainless-steel plates and pressed into glass flakes. Subsequently, the pressed glasses sheets were annealed at 500 °C for 2 h to relieve the thermal stresses, followed by cooling the furnace to room temperature. Finally, the obtained glasses ceramics plates were sliced into the 0.6 mm thick plate, then the plates were carefully polished to the required thickness of approximately 0.3 mm.

Preparation of the LAGP modified Separator

The coating of routine PP separator with LAGP ceramic powder (referred as LAGP modified separator) was performed by a simple casting procedure. 0.5g PVDF was used as a binder in a solvent of 8 g *N*-methyl pyrrolidone (NMP). Then 9.5 g of LAGP ceramic powder was gradually added into the above solution. After vigorous mixing, the paste was coated onto one side of the pristine PP separator with a thickness of ca. 20 μm . The LAGP modified separator was obtained after it was dried naturally at room temperature and then dried at 50 °C for 24 h under vacuum for the evaporation of NMP.

The ionomer electrolyte was composed of the LAGP modified separator and liquid electrolyte. A solution of 1.0 M $\text{LiN}(\text{CF}_3\text{SO}_2)_2$ in dioxolane (DOL) and dimethoxyethane (DME) (1:1 v/v) mixture was used as liquid electrolyte.

Preparation of the Sulfur cathode

The S/C composite was prepared by planetary ball milling with a mixture of sulfur, Ketjen black and Super P, in the weight ratio of 6:1:1. Then the composite was sealed in a reaction axe followed by co-heating at 155 °C for 12 h. Consequently, the slurry was prepared by ball milling with 80 wt.% S/C composite, 10 wt.% Vapor-grown carbon fiber conductive agent, 10 wt.% LA133 binders, and deionized water solvent. The slurry was casted onto aluminum foil substrates using a doctor blade. After the solvent was evaporated, the electrode was cut into discs with 16 mm in diameter and then dried at 50 °C under vacuum for 12 h. The thickness of the sulfur electrode is ca. 48 μm .

Characterization

Powder X-ray diffraction (XRD, Rigaku3014) using $\text{Cu-K}\alpha$ radiation was employed to identify the crystalline phase of the sintered LAGP glass ceramic. Scanning electron microscope (SEM) was

performed using JSM S4800 (JEOL Ltd.) to analyze the morphology of the LAGP glass ceramic plate, modified separator and the Li pellet, respectively. To qualitatively analyze the lithium polysulfides in the electrolyte in both sides of the cathode and the anode, Raman spectrometry (DXR Raman Microscope, Thermo Fisher Scientific) with a frequency diode laser at 532 nm was used. The LiTFSI/DOL+DME contact angles on the routine separator, LAGP modified separator, and LAGP glass ceramic plate were determined by the contact angle measurement system (Dataphysics, OCA20, Germany) at 25 °C. Simultaneously, we employed the air permeability test to evaluate the compactness of the LAGP modified separator.

Electrochemical measurements

The different ionic conductivities of the PP separator, the LAGP modified separator as well as the LAGP glass ceramic plate are compared in detail. Prior to the measurement for the LAGP plate, Au was sputtered onto both sides of the LAGP plate to ensure electrical contact as the blocking electrode. However, the PP separator and the LAGP modified separator were placed between the stainless steel sheets, and the ionic conductivity measurement was conducted in the 1 M LiTFSI/DOL+DME solution.

Li-ion transference number of the LAGP modified separator was determined by using the steady-state current method,³² on a cell assembled by sandwiching the electrolyte between two Li-In alloys. The method consists of initial measurement of the Li-In alloy interfacial resistance (R_0), then application of a small voltage (ΔV , 10 mV) until a steady current (I_{ss}) is obtained, and final measurement of the interfacial resistance (R_f). Li-ion transference number (t_{Li^+}) is calculated using the equation of $t_{Li^+} = [I_{ss} (\Delta V - I_0 R_0)] / [I_0 (\Delta V - I_{ss} R_f)]$, where I_0 is the initial current.

The basic physical parameters of the H type cell are as follows: 6 cm in length, height 8 cm, and the glass inner diameter is 1.2 cm. In addition, the amount of the electrolyte is approximately 12 ml. The H type cells were assembled in an Argon-filled glove box, and the binder was used to seal. The rectangular shape sulfur electrode is chosen as the cathode and the sulfur loading per unit area is 2.1 mg cm⁻², the weight of sulfur on the cathode is approximately 4.2 mg. The lithium foil (50 μm) is used as the anode. And the separator is LAGP glass ceramic plate, LAGP modified separator and microporous PP membrane, respectively.

To conduct the galvanostatic charge/discharge tests, the CR2430-type coin cells were assembled in an Argon-filled glove box. Sulfur electrodes were punched into round disks with a diameter of 16 mm. And the element S loading on the cathode is approximately 4.2 mg (2.1 mg cm⁻²). Lithium foil (50 μm)

was used as the counter and reference electrode, the microporous PP membrane or LAGP modified separator as separator. Galvanostatic charge/discharge tests were performed at a current density of $100 \text{ mA}\cdot\text{g}^{-1}$ (0.42 mA) in the potential range of 1.7 V - 2.5 V (vs. Li/Li^+) at $25 \text{ }^\circ\text{C}$ by using a LAND CT2001A (Wuhan, China) battery-testing instrument. In order to investigate the effect of LiNO_3 additive on the efficiency of the battery, two kinds of the electrolyte were used: $1 \text{ M LiTFSI/DOL+DME}$ ($1:1, \text{ v/v}$) and $1 \text{ M LiTFSI/DOL+DME}$ ($1:1, \text{ v/v}$) containing 0.4 M LiNO_3 , respectively. $50 \text{ }\mu\text{L}$ of the electrolyte was injected ($11.9 \text{ }\mu\text{L}/\text{mg}$ [S]) in the coin cells. The specific capacity was calculated on the basis of the weight of sulfur on the cathode.

To figure out the effect of the LAGP modified layer on suppressing the polysulfides, electrochemical impedance spectroscopy (EIS) analysis of lithium electrode are carried out using Solartron electrochemical station in the form of three-electrode mold. And the fresh lithium disc or the cycled lithium electrodes are used as working electrodes another two lithium foils are used as counter electrode and reference electrode, respectively

3. Results and discussion

In this part, we characterize a series of physical and chemical properties of the LAGP, observe its suppressing diffusion effect of the polysulfides, and then conduct the discharge of the H-type visible battery. On the basis of above works, the LAGP modified separator is developed and used in the subsequent electrochemical tests.

XRD pattern of the as-prepared LAGP glass ceramic is given in Fig. 1. Apart from a small amount of AlPO_4 , all the diffraction peaks of the specimen are well matched with NASICON $\text{LiGe}_2(\text{PO}_4)_3$ (JCPDS 80-1924) structure, indicating that NASICON-type phases are obtained in LAGP particles. It's well known that the NASICON-type structure could provide suitable tunnels for lithium ion migration in the LAGP electrolyte. Although 25% of Ge has been substituted by Al, the diffraction peaks show a slight shift, attributing to the similarity in ionic radius between Ge^{4+} (53 pm) and Al^{3+} (51 pm). Synthesis of LAGP by a solid-state reaction brings impurity like AlPO_4 due to the reaction of Al^{3+} and PO_4^{3-} . According to the related work,³³ this insulating dielectric material improves the lithium ion conductivity of solid electrolyte.

The SEM images of surface and fracture surface of the LAGP glass ceramic plate calcined at 1350°C for 2h are shown in Fig.2a and Fig.2b. As displayed in surface, the microstructure of the LAGP glass-ceramic plate shows a narrow crystal size distribution ranging from 0.1 to $0.7 \text{ }\mu\text{m}$. In addition,

from the microstructure for the fracture surface of the glass ceramic, it is apparent that a well close packing is achieved between the particles of the glass ceramic plate, eliminating the existence of opening holes. Accordingly, the dense glass ceramic plate is promising to apply in Li-S cells for blocking the diffusion of Li_2S_x ($2 < x \leq 8$) during charge/discharge process.

A comparison of the optical images of polysulfides diffusion between the PP separator, the modified separator and the LAGP glass ceramic plate is presented in Fig.3, in which 0.025M long chained S_6^{2-} is distributed in the electrolyte (1 M LiTFSI / DOL+DME (1:1, v/v)). As is expected, the common PP separator can not suppress the diffusion of lithium polysulfides. Thus, the color of the transparent electrolyte already changes from colorless to yellow after 30 minutes (Fig.3a), indicating the diffusion of a little amount chained-like polysulfides. After 3 hours (Fig.3b), especially, after 50 hours (Fig.3c), a concentrated orange solution is obtained due to diffusion of chained-like polysulfides from the reservoir through the separator. In contrast, in Fig.3d-f, the same measurement is conducted with LAGP modified separator. No obvious change of the color in the right chamber can be observed even after standing for 3 hours (Fig.3e). However, after standing for 50 hours, a light yellow solution appears (Fig.3f), which suggests that the LAGP modified separator, with time increasing, could not block the polysulfides effectively from diffusing away. It indicates that the prepared LAGP modified separator is not dense. As comparison, clearly, after 50 hours of rest, the electrolyte with the dense LAGP glass ceramic plate remains colorless (Fig.3i), suggesting the dense LAGP glass ceramic plate can shut down the diffusion path of polysulfides. It can be attributed to the compactness of LAGP glass ceramic plate in which Li^+ ion is admitted to pass through.

For the purpose of current collection in H type cell, the rectangular shape sulfur electrode is chosen. H type cells based on LAGP glass ceramic plate as well as PP separator have initial discharge capacities of approximately 974.5 mAh g^{-1} and 721.1 mAh g^{-1} at $35 \mu\text{A}$, respectively (Fig.4a). Clearly, the glass ceramic plate improves the utilization of the sulfur electrode. Fig.4 b presents the optical image of the discharge to the 50 h. Clearly, no obvious change of the color in the lithium anode chamber can be observed even after working for 50 h, which can be supported in Fig.3i, and further confirms that the LAGP glass ceramic plate shuts down the diffusion of lithium polysulfides. As comparison, the same measurement is performed with routine PP separator. The original transparent colorless liquid becomes light yellow for the anolyte after 50 h, which indicates fast diffusion process of polysulfides. As depicted in Fig.4c, the catholyte and the anolyte of the visible H type cells are

collected after discharging. In the case of the PP separator, the color of the catholyte and anolyte is both changed to yellow, implying the concentration balance of polysulfides between catholyte and anolyte. However, while the anolyte of cell using the LAGP glass ceramic plate remains transparent, the catholyte of that is also changed to yellow. The above results directly indicate that the dense LAGP glass ceramic plate blocks polysulfides diffusion to the anode.

In order to further evaluate the effectiveness of the LAGP glass ceramic plate, Raman spectroscopy is applied to analyze the above electrolyte. Fig.5a and Fig.5b exhibit comparative Raman results of the catholyte and the anolyte before and after discharging of Li-S cell using the routine PP separator and dense LAGP glass ceramic plate, respectively. The fresh electrolyte presents prominent peaks at 314, 348, 759, 942, 1043, 1231, 1477, 2765, 2891 and 2955 cm^{-1} .²⁰ For the cell using PP separator (in Fig.5a), the intensity of the above peaks significantly decreases for the catholyte and the anolyte after discharging. Especially, the pristine strong peaks at 1043, 1477 and 2891 cm^{-1} observed in the electrolyte weakened after the testing. In addition, broad peaks, on behalf of lithium polysulfide, appear at approximately 2200 and 2500 cm^{-1} .²⁰ For the cell using LAGP glass ceramic plate (in Fig. 5b), as above, the strong peaks at 1043, 1477 and 2891 cm^{-1} in the catholyte is also weakened, and the broad weak peaks of lithium polysulfide are visible. However, the peaks intensity of the electrolyte in the anode side of the cell using LAGP glass ceramic plate after discharging remains changeless, and the broad peaks assigned to lithium polysulfide doesn't appear. Additionally, the differences of Raman spectroscopy between the anolyte and the catholyte, further verify that the dense LAGP glass ceramic plate shuts down the diffusion of lithium polysulfides to the lithium anode.

The above works about the diffusion of polysulfides and the utilization of the sulfur electrode are necessary, which confirms LAGP glass ceramic plate can shut down the diffusion of S_x^{2-} ions and enhance the utilization ratio of sulfur electrode. That lays the foundation for the further application of LAGP. However, despite the solid electrolyte of LAGP has a good performance in blocking the migration of Li_2S_x ($2 < x \leq 6$), as well as improving the utilization of sulfur electrode, but in fact, it is difficult to be processed into flexible membrane due to its brittle and fragile properties, which greatly restricted its application in Li-S battery. So the LAGP modified separator is employed in the subsequent electrochemical tests, not the LAGP glass ceramic plate. Another problem is the reactivity of lithium metal toward LAGP, some researchers have different views on it.³⁴⁻³⁶ So it was precluded the use of LAGP in direct contact with a Li anode in our experiment.

Fig. 6 shows the fracture surface images of the LAGP modified separator that seems to be a close-packed arrangement. The thickness of the PP separator is approximately 23.8 μm and the thickness of the coating layer is about 27.8 μm . Gurley value is often chosen to quantitatively characterize the pore size, distribution, and porosity of the separators in the air permeability test. Generally, the high Gurley value corresponds to a long tortuous path for air permeability.³⁷ As shown in Table 1, the Gurley value of the routine PP separator (40 μm) is 647.1 s 100 ml⁻¹ (0.02 MPa, 0.79 cm²) while the Gurley value sharply increases to 2102.3 s.100 ml⁻¹ for the LAGP modified separator (51.6 μm). It can be inferred the less interstitial voids formed between the LAGP particles in the coating layer. The voids will increase the internal resistance of the Li-S cells, but effectively decrease the diffusion path of lithium polysulfides, thus improve the electrochemical performance.

To identify the wettability of the separators, the contact angle of the electrolyte on the different separators is determined. As shown in Table 1, compared with the 27.47° for the PP separator, the LAGP modified separator shows a contact angle of 20.48°, suggesting that the introduction of the solid electrolyte powder makes the modified separator more easily wetted by the electrolyte solution.

The outcomes of using steady-state current method to measure t_{Li^+} of the electrolyte in the LAGP modified separator are shown in Fig. 7a. Parameters obtained for t_{Li^+} calculation are: $I_{\text{ss}} = 40.7 \mu\text{A}$, $I_0 = 47.2 \mu\text{A}$, $R_0 = 137.8 \Omega$, $R_f = 162.9 \Omega$. It is calculated that t_{Li^+} is 0.895, indicating that the modified layer could effectively improve the lithium ion transference number

As shown in Fig.7b, the Nyquist plots of the separators are straight lines, indicating that the current carriers are ions and the total conductivity is the ion conductivity.³⁸ The intercept of the straight line with the real axis is the bulk impedance. Since the resistance for lithium ion transport in the solid electrolyte layer is larger than that in the liquid electrolyte, the bulk impedance increases when the inorganic electrolyte layer is introduced.³⁹ As shown in Fig.7c, compared with the PP membrane ($1.002 \times 10^{-3} \text{ S cm}^{-1}$), the ionic conductivity of the LAGP modified PP is only $6.280 \times 10^{-4} \text{ S cm}^{-1}$ in 1 M LiTFSI/DOL+DME solution, which is larger than that of the LAGP glass ceramic plate ($3.130 \times 10^{-4} \text{ S cm}^{-1}$), suggesting that the LAGP modified separator exhibits an acceptable ion conductive behavior in the electrolyte. Fig.7d shows the Arrhenius plots of total conductivity, σ_t , in the -3 to 70 °C temperature range for the LAGP glass-ceramic plate and LAGP modified separator. The dots are experimental data, and the two lines are their Arrhenius fitting curves. The Arrhenius plots of the specimens are linear and the conductivity data fit the Arrhenius equation of $\sigma_t = A \exp[-E_a/(\kappa_B T)]$, where A is the pre-exponential

term, E_a is the activation energy for conduction and κ_B is Boltzmann's constant and T is the absolute temperature. It is found that the E_a of LAGP glass ceramic plate is 0.28 eV, while the one of the modified separator is only 0.17 eV, suggesting that the energy barrier for the LAGP modified separator of Li^+ transport is lowered, compared with solid electrolyte of LAGP glass ceramic plate.

In order to investigate the effect of different separator on the coulombic efficiency, galvanostatic charge/discharge was carried out at the current rate of 100 mA g^{-1} (0.42 mA) between 1.7 and 2.5 V vs. Li/Li^+ . For control experiment, 0.4M Lithium nitrate additive was not added into the electrolyte. Fig.8a and Fig.8b present typical charge/discharge voltage profiles of electrodes using PP separator and LAGP modified separator, respectively. As shown in Fig.8a, it is found that the Li-S cell using routine PP separator delivers a discharge capacity of 973.3 mAh g^{-1} and a charge capacity of 2598.5 mAh g^{-1} , leading to a low Coulombic efficiency of 37.4 %. This phenomenon can be attributed to, at the absence of LiNO_3 additive, the dissolved chained-like polysulfides anions during discharge in the electrolyte which give rise to a redox shuttle effect inside the cell due to their spontaneous reduction and oxidation and freely diffusion in the electrolyte from S cathode to Li anode. It indicates that an over-charge is needed to reach full charge condition. From the charge capacity of 2055.3 mAh g^{-1} and the discharge capacity of 810.6 mAh g^{-1} in the second cycle, it can be seen that the over-charge is almost-153%, meaning a high electric energy waste. The cell using the LAGP modified separator, by contrast, delivers a discharge capacity of 1130.2 mAh g^{-1} and a charge capacity of 1258.1mAh g^{-1} in the initial cycle as shown in Fig.8b. The Coulombic efficiency is as high as 89.8 %. As shown in Fig.9, the performance of the batteries presents a capacity decline, using routine PP separator or LAGP modified separator. An interesting phenomenon is that the coulombic efficiency of Li-S cell using PP separator presents a relative growth momentum in initial 20 cycles, whereas, Li-S cell using the modified separator displays stable coulombic efficiency. The above results suggest that the introduction of the LAGP modified layer can effectively suppress the shuttle phenomenon of polysulfides.

To demonstrate the electrochemical performance of the Li-S cell using the LAGP modified separator, typical charge/discharge test was performed at the current of 0.42 mA (100 mA g^{-1}) between 1.7 and 2.5 V. 0.4M lithium nitrate (LiNO_3) dissolved in the above mentioned DOL/DME with 1M LiTFSI electrolyte was employed. Fig.10a and Fig.10b present charge/discharge voltage profiles of Li-S cells with or without LAGP modified layer from 1st to 50 th cycle, respectively. It is found that the cell using LAGP modified separator shows higher charge voltage plateau and lower discharge voltage

plateau than that of the cells using conventional PP separator, especially, it is observed an enlarged polarization in the first two discharge curves, which is in agreement with the large impedance and the Gurley value of the LAGP modified separator.

As shown in Fig.11, the initial discharge capacity is approximately $1128.2 \text{ mAh g}^{-1}$ for the cell using LAGP modified separator. However, the first discharge capacity is only 958.3 mAh g^{-1} for that using PP separator. After 50 cycles, unfortunately, the discharge capacities obtained from the LAGP modified separator and the normal PP separator suffers a sharp decrease to 770.1 mAh g^{-1} and 658.4 mAh g^{-1} , respectively. Combining the LAGP modified layer and LiNO_3 additive, the coulombic efficiency of the cells using the LAGP modified separator is higher than that using PP separator in initial cycles. And such a trend has not changed in the subsequent cycles. Obviously, the introduction of LAGP modified layer can improve the utilization of sulfur electrode, though the cycle performance does not improve markedly. The cycle performance will be improved by optimizing the preparation technology of the LAGP modified separator and S/C composite electrode, and protecting the lithium anode from the reaction of polysulfides, which will be studied at the next stage of the related work.

To figure out the effect of the LAGP modified layer on suppressing the polysulfides, electrochemical impedance spectroscopy (EIS) analysis of lithium electrode are carried out using Solartron electrochemical station in the form of three-electrode mold. And the fresh lithium disc or the cycled lithium electrodes are used as working electrodes, respectively. Additionally, both the counter electrode and the reference electrode were the fresh lithium metal. The Nyquist plots of lithium electrode with the routine PP separator and the LAGP modified separator are displayed in Fig.12. Generally, the Nyquist plots of lithium electrode consist of reaction impedance (high frequency region) and SEI film impedance (low frequency region),¹⁷ and the equivalent circuits of these lithium electrodes are shown in the inset of Fig.12. The fitted values of the impedance spectra in Fig. 12 are summarized in Table 2. It is clear that the charge transfer resistance (reaction resistance) has little change, while the change of the impedance is mainly derived from the SEI impedance. The SEI impedance of lithium anode with PP separator is increased from 15.33Ω to 28.31Ω after 50 cycles, while the film impedance is only increased to 20.26Ω for the use of the LAGP modified separator. Accordingly, the result is quit in line with the superior utilization of sulfur electrode shown by the LAGP modified separator.

Generally, the discharge current has considerable impacts on the deposition morphology and lithium metal will form dendrites at current densities higher than $1\text{-}2 \text{ mA cm}^{-2}$ during cycling.⁴⁰ Moreover, it's

worth mentioning that the impact factors on the morphology of the deposited Li are affected by the composition and concentration of organic solvents, the composition and concentration of lithium salts, electrolyte additives, as well as the current collector, etc.⁴¹⁻⁴³ Therefore, the dendrites formation phenomenon can be ignored, because the coin cells used in this work were operated at the same current density of 0.21 mA cm^{-2} , and other test conditions are the same. As shown in Fig.13a, the surface morphology of the fresh lithium sheet is smooth, while it exposes much loose deposits after 50 cycles (Fig.13b), which indicate that the formed lithium polysulfides accumulated on the surface of lithium anode for the cell of using PP separator, thus, the lithium anode suffered serious corrosion during charge/discharge process. However, the surface of lithium anode, with the introduction of LAGP modified layer, is relatively flat and uniform (Fig.13c), suggesting that the addition of LAGP modified layer effectively suppress the diffusion of lithium polysulfides between the electrodes.

4. Conclusion

In summary, the LAGP was used in this paper to improve the electrochemical performance of Li-S battery. Compared with the routine PP separator, the LAGP modified separator shows more satisfactory wettability, Gurley value, as well as Li^+ transference number. The electrochemical analysis shows that the LAGP modified separator delivers the initial discharge capacity of $1128.2 \text{ mAh g}^{-1}$, which is 169 mAh g^{-1} higher than that of the Li-S cells with PP separator. After 50 cycles, the discharge capacity of 770 mA h g^{-1} can be maintained by using the modified separator. The LAGP modified separator is a suitable method for overcoming the shuttle phenomenon of Li-S cells. Additionally, improving the compactness and the stability without increasing the thickness of LAGP modified layer, is a promising method to further enhance the electrochemical capacity and cycle performance by inhibiting the migration of lithium polysulfides to the anode side in Li-S cells.

References

- 1 A. Manthiram, Y. Fu, Y.-S. Su, *Acc. Chem. Res.*, 2012, 46, 1125-1134.
- 2 X.-B. Cheng, J.-Q. Huang, H.-J. Peng, J.-Q. Nie, X.-Y. Liu, Q. Zhang, F. Wei, *J. Power Sources*, 2014,

- 253, 263-268.
- 3 S.-R. Chen, F. Dai, M.-L. Gordin and D.-H. Wang, *RSC Adv.*, 2013, 3, 3540–3543.
- 4 M.-S. Park, J.-S. Yu, K.-J. Kim, G.-J. Jeong, J.-H. Kim, T. Yim, Y.-N. Jo, S. Kang, T.-W. Woo, H.-S. Kim and Y.-J. Kim, *RSC Adv.*, 2013, 3, 11774-11781.
- 5 M. Oschatz, S. Thieme, L. Borchardt, M. Lohe, *Chem. Commun.*, 2013, 49, 5832-5834.
- 6 S. Evers, T. Yim, L. Nazar, *J. Phys. Chem. C.*, 2012, 116, 19653-19658.
- 7 R.D. Cakan, M. Morcrette, F. Nouar, C. Davoisne, T. Devic, D. Gonbeau, R. Dominko, C. Serre, G. Féréy, J.M. Tarascon, *J. Am. Chem. Soc.*, 2011, 133, 16154-16160.
- 8 W. Li, Q. Zhang, G. Zheng, Z.-W. Seh, H. Yao, Y. Cui, *Nano Lett.*, 2013, 13, 5534 -5540.
- 9 G. C. Li, G.-R. Li, S.-H. Ye, X.-P. Gao, *Adv. Energy Mater.*, 2012, 2, 1238-1245.
- 10 S.S. Zhang, *J. Electrochem. Soc.*, 2012, 159, A920-A923.
- 11 D. Aurbach, E. Pollak, R. Elazari, G. Salitra, *J. Electrochem. Soc.*, 2009, 156, A694-A702.
- 12 S.S. Zhang, *Electrochim. Acta*, 2013, 97, 226-230.
- 13 S.S. Zhang, *Electrochim. Acta*, 2012, 70, 344-348.
- 14 N. Yan, X.-F. Yang, W. Zhou, H.-Z. Zhang, X.-F. Li and H.-M. Zhang, *RSC Adv.*, 2015, 5, 26273-26280.
- 15 J. Balach, T. Jaumann, M. Klose, S. Oswald, J. Eckert, L. Giebeler, *J. Phys. Chem. C.*, 2015, 119, 4580-4587.
- 16 Y.-S. Su, A. Manthiram, *Chem. Commun.*, 2012, 48, 8817-8819.
- 17 G.-Q. Ma, Zh.-Y. Wen, Q.-S. Wang, C. Shen, P. Peng, J. Jin, X.-W. Wu, *J. Power Sources*, 2015, 273, 511-516.
- 18 C. Zu, Y.-S. Su, Y. Fu, A. Manthiram, *Phys. Chem. Chem. Phys.*, 2013, 15, 2291-2297.
- 19 X. Wang, Z. Wang, L. Chen, *J. Power Sources*, 2013, 242, 65-69.
- 20 W. Ahn, S.N. Lim, D.U. Lee, K.B. Kim, Z.-w. Chen, S.H. Yeon, *J. Mater. Chem. A.*, 2015, 3, 9461-9467.
- 21 Z.-Y. Zhang, Y.-Q. Lai, Z.-A. Zhang, K. Zhang, J. Li, *Electrochim. Acta*, 2014, 129, 55-61.
- 22 I. Bauer, S. Thieme, J. Brückner, H. Althues, S. Kaskel, *J. Power Sources.*, 2014, 251, 417-422.
- 23 G.-H. Wang, Y.-Q. Lai, Z.-A. Zhang, J. Li, *J. Mater. Chem. A.*, 2015, 3, 7139-7144.
- 24 Y.-G. Sun, *Nano Energy.*, 2013, 2, 801-806.
- 25 X.-X. Xu, Z.-Y. Wen, X.-W. Wu, X.-L. Yang, Z.-H. Gu, *J. Am. Ceram. Soc.*, 2007, 9, 2802-2806.

- 26 Q.-S. Wang, J. Lin, X.-W. Wu, G.-Q. Ma, J.-H. Yang and Z.-Y. Wen, *Phys. Chem. Chem. Phys.*, 2014, 16, 21225-21229.
- 27 Q.-S. Wang, Z.-Y. Wen, J. Lin, J. Guo, et al, *Chem. Commun.*, 2016, 52, 1637-1640.
- 28 X.-W. Yu, Z.-H. Bi, F. Zhao, and A. Manthiram, *Appl. Mater. Interfaces*, 2015, 7, 16625-16631.
- 29 L.-N. Wang, Y.-G. Wang and Y.-Y. Xia, *Energy Environ. Sci.*, 2015, 8, 1551-1558.
- 30 N. Li, Z. Weng, Y.-R. Wang, F. Li, H.-M. Cheng, and H.-S. Zhou, *Energy Environ. Sci.*, 2014, 7, 3307-3312.
- 31 Q.-S. Wang, Z.-Y. Wen, J.-H. Yang, J. Jin, X. Huang, X.-W. Wu, J.-D. Han, *J. Power Sources*, 2016, 306, 347-353.
- 32 Z.-Q. Jin, K. Xie, X.-B. Hong, Z.-Q. Hu, X. Liu, *J. Power Sources*, 2012, 218, 163-167.
- 33 J. S. Thokchom, B. Kumar, *J. Power Sources*, 2010, 19, 2870-2876.
- 34 P. Hartmann, T. Leichtweiss, M. R. Busche, et al, *J. Phys. Chem. C.*, 2013, 117, 21064-21074.
- 35 M. Kotobuki, K. Hoshina, K. Kanamura, *Solid State Ionics*, 2011, 198, 22-25.
- 36 J.-K. Feng, L. Lu, M.-O. Lai, *J. Alloys and Compounds*, 2010, 501, 255-258.
- 37 J.-L. Shi, H.-S. Hu, Y.-G. Xia, Y.-Z. Liu, Z.-P. Liu, *J. Mater. Chem. A.*, 2014, 2, 9134-9141.
- 38 Y.-S. Zhu, F.-X. Wang, L.-L. Liu, S.-Y. Xiao, Z. Chang, Y.-P. Wu, *Energy Environ. Sci.*, 2013, 6, 618-624.
- 39 J.-Y. Kim, S.-K. Kim, S.-J. Lee, S.-Y. Lee, H.-M. Lee, S. Ahn, *Electrochim. Acta*, 2004, 50, 363-366.
- 40 I.-W. Seong, C.-H. Hong, B.-K. Kim, W.-Y. Yoon, *J. Power Sources*, 2008, 178, 769-773.
- 41 O. Crowther, A.C. West, *J. Electrochem. Soc.*, 2008, 155, A806-A811.
- 42 D. Aurbach, Y. Cohen, *J. Electrochem. Soc.*, 1997, 144, 3355-3360.
- 43 S.-K. Jeong, H.-Y. Seo, D.-H. Kim, H.-K. Han, J.-G. Kim, Y.B. Lee, Y. Iriyama, T. Abe, Z. Ogumi, *Electrochem. Commun.*, 2008, 10, 635-638.

Figure captions

Fig.1 X-ray diffraction patterns of the specimens for LAGP glass ceramic treated at 1350 °C for 2 h.

Fig.2 Scanning electron microscope images of the surface (a) and fracture surface (b) morphology of the LAGP glass ceramic plate.

Fig.3 The optical images of the diffusion process of polysulfides of PP separator (a-c), LAGP modified

separator (d-f) and LAGP glass ceramic plate (g-i) in H type cell after variable resting times.

Fig.4 Discharge curves of Li-S cells using the LAGP glass ceramic plate and PP separator (a), the optical image of the discharge to the 50 h (b), and the color change comparison of the catholyte and the anolyte (c).

Fig.5 Raman study results for the electrolyte using (a) the PP separator before the electrochemical test and after the test; (b) the LAGP glass ceramic plate before the electrochemical test and after the test.

Fig.6 Scanning electron microscope image of the fracture surface of the LAGP modified separator.

Fig.7 Chronoamperometry of the Li-In/LAGP modified separator/Li-In cell at a potential step of 10 mV. Insert: the AC impedance spectra of the same cell before polarization and after the steady-state current (a), the Nyquist plots of PP, LAGP glass ceramic plate, LAGP modified separator (b), the ion conductivity of the PP, LAGP glass ceramic plate, and LAGP modified separator at 25 °C, respectively, (c), and Arrhenius plots of the total conductivity for the LAGP glass ceramic plate and modified separator at different temperatures (d).

Fig.8 The Galvanostatic charge/discharge profiles of Li-S cells using the routine PP separator (a) and LAGP modified separator (b). The cells were assembled with the electrolyte DOL/DME (1:1, v:v) containing 1 M LiTFSI.

Fig.9 Cycle performance and Coulombic efficiency comparisons of electrodes using PP separator and LAGP modified separator.

Fig.10 Charge/discharge curves of Li-S cells using the routine PP separator (a) and LAGP modified separator (b). 0.4M lithium nitrate (LiNO_3) dissolved in the above mentioned DOL/DME with 1 mol L^{-1} LiTFSI electrolyte was employed.

Fig.11 Comparison of cycle performance and coulombic efficiency using the routine PP separator and LAGP modified separator at 100 mA g^{-1} .

Fig.12 EIS spectra of Lithium electrode with PP, LAGP modified separator after 50 cycles.

Fig.13 The SEM image of the fresh Li anode (a), the Li anode after 50 cycles with PP separator (b), and the Li anode after 50 cycles with LAGP modified separator (c).

Table 1 Comparison of the basic physical parameters of the PP, LAGP modified separator, LAGP glass ceramic plate

Table 2 Fitted values of the impedance spectra in Fig.12

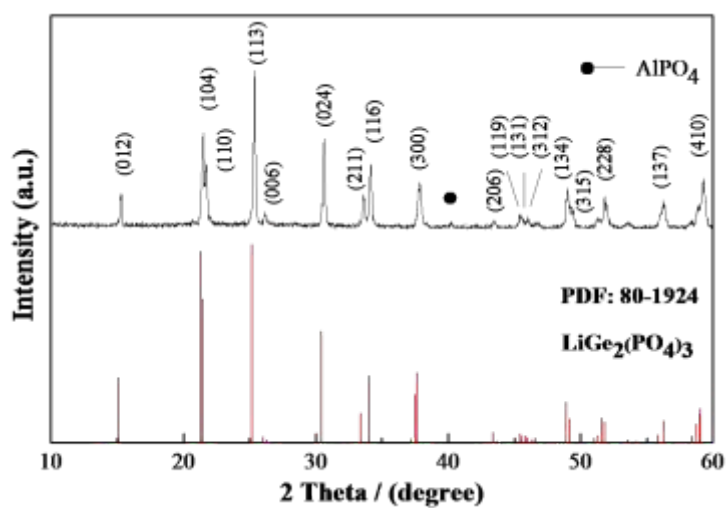


Fig.1

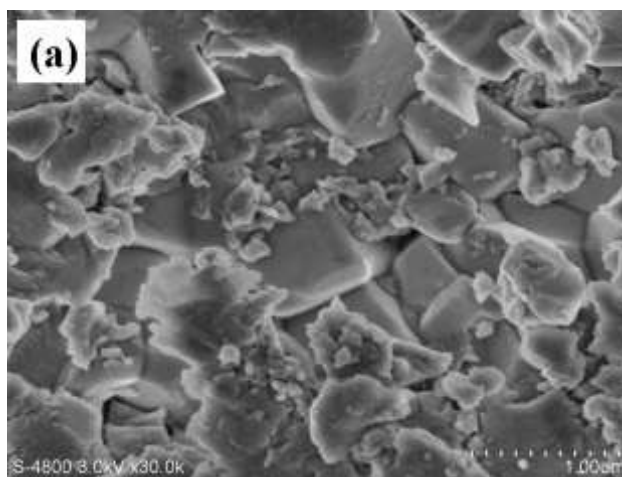


Fig.2a

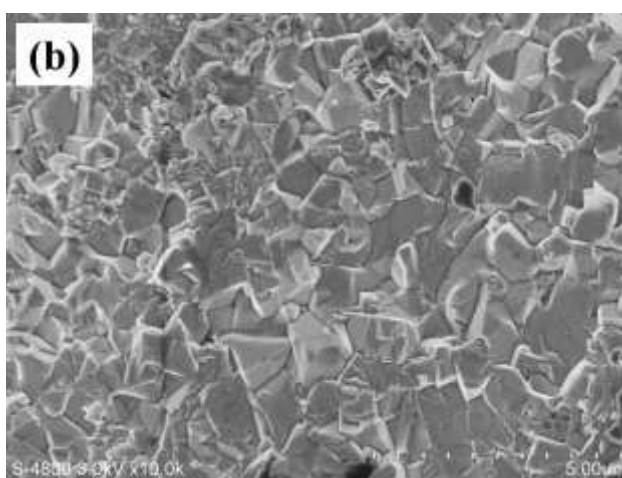


Fig.2b

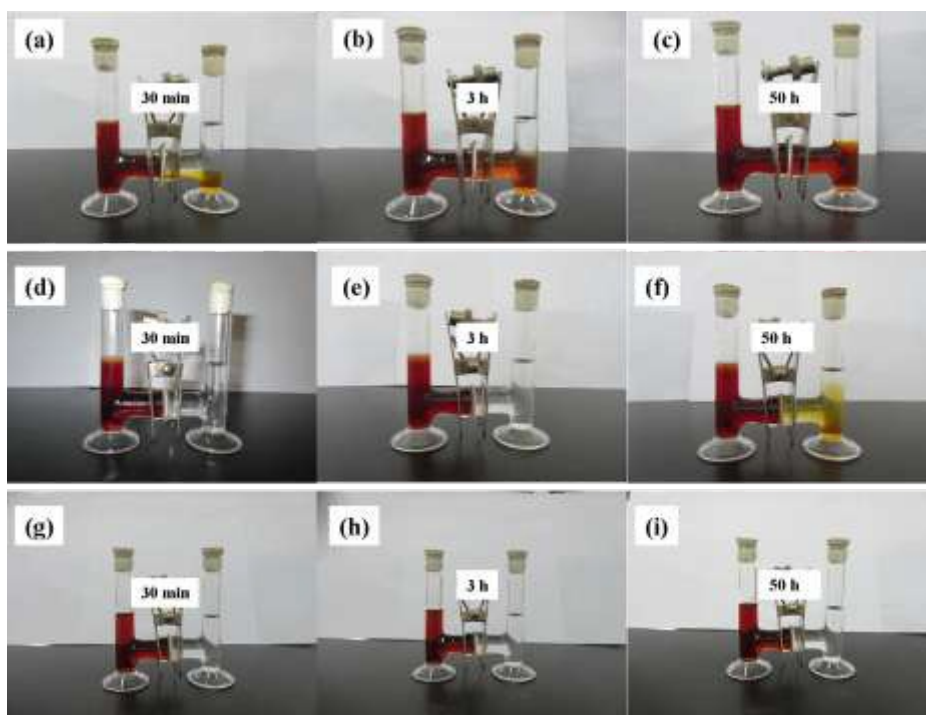


Fig.3

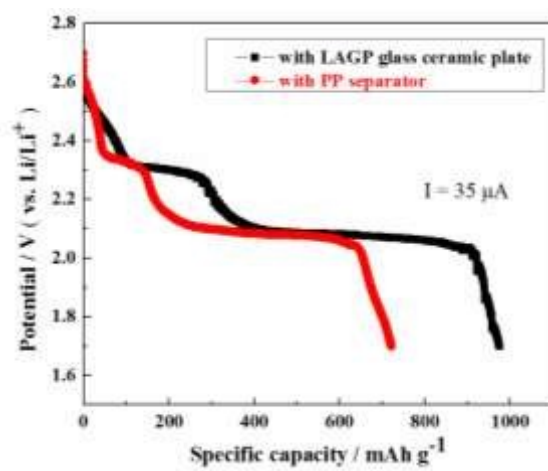


Fig.4a

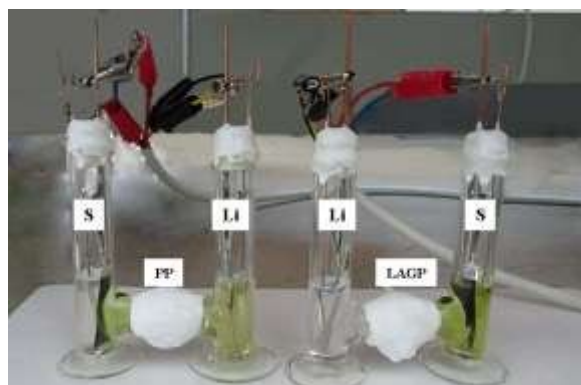


Fig.4b

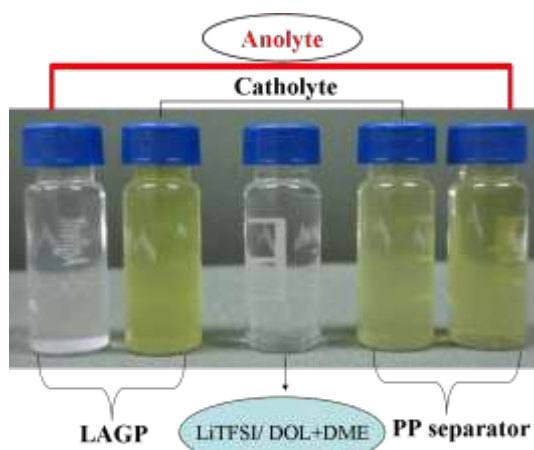


Fig.4c

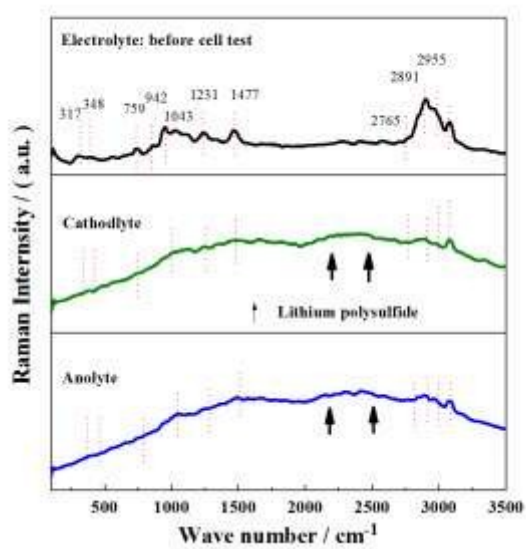


Fig.5a

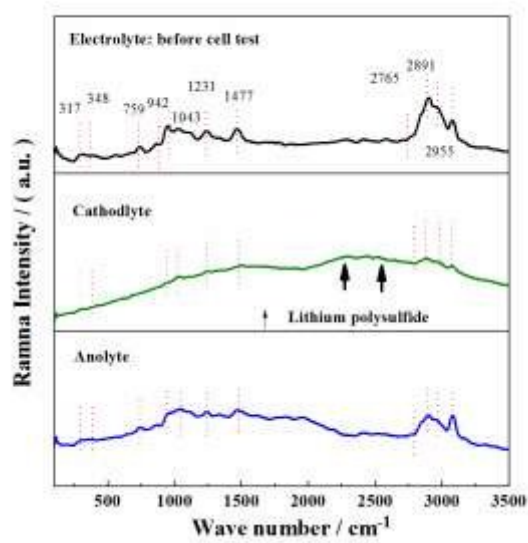


Fig.5b

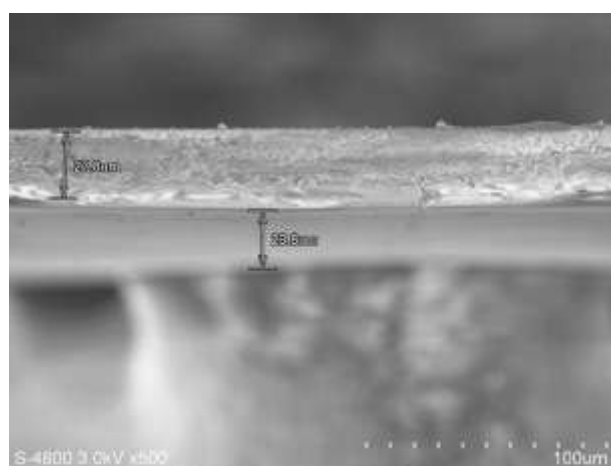


Fig. 6

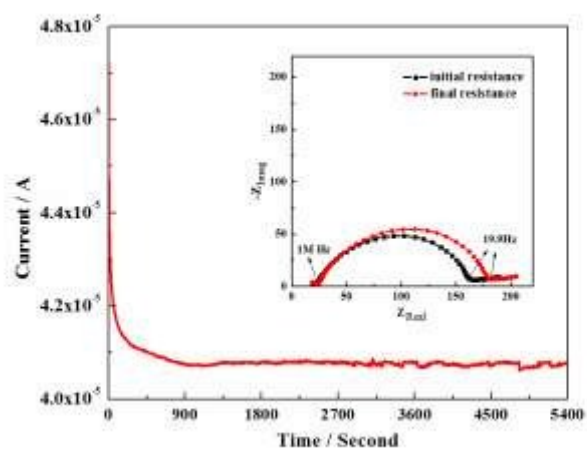


Fig.7a

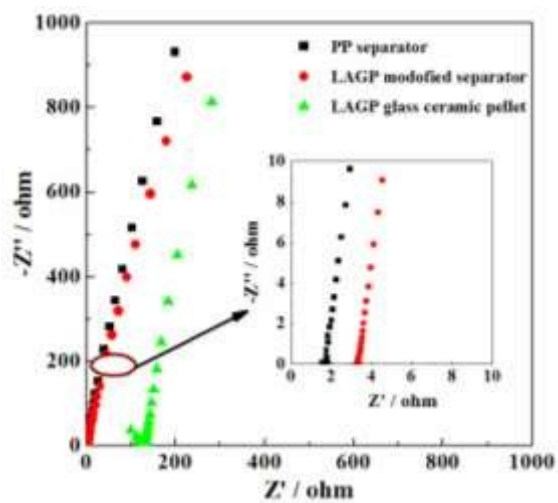


Fig.7b

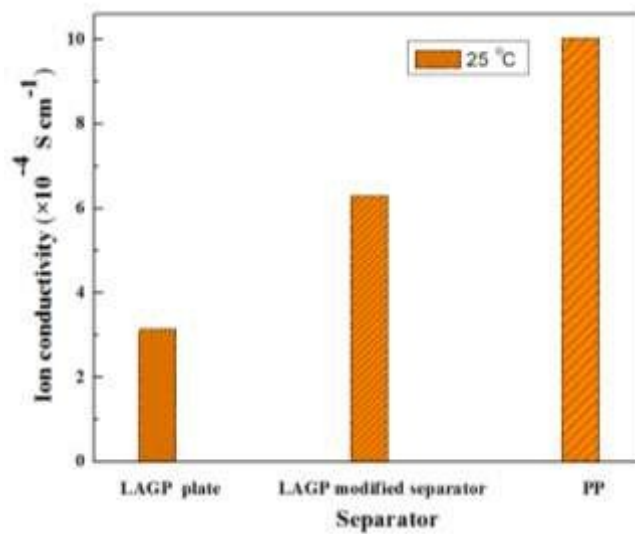


Fig.7c

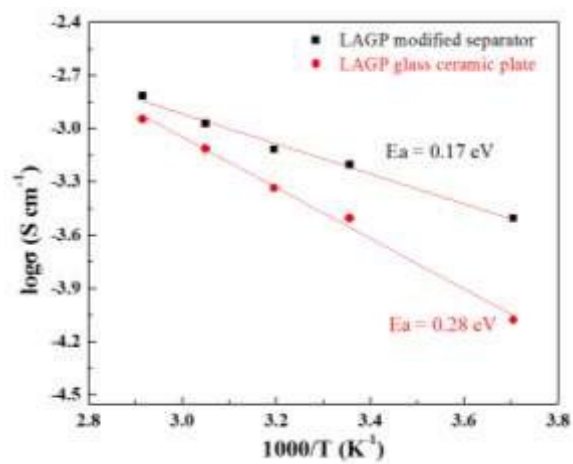


Fig.7d

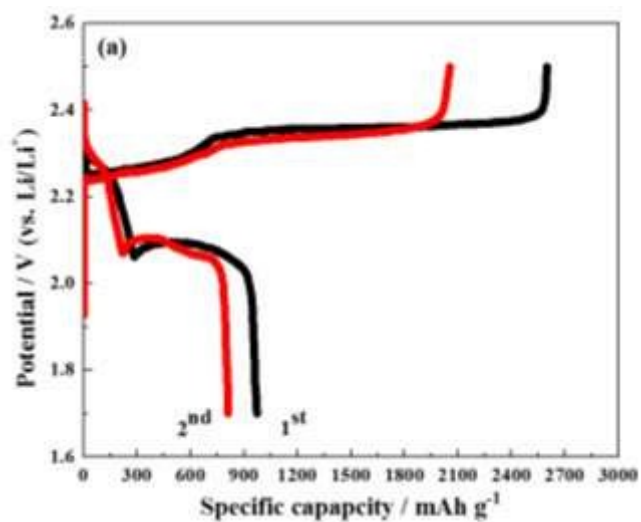


Fig.8a

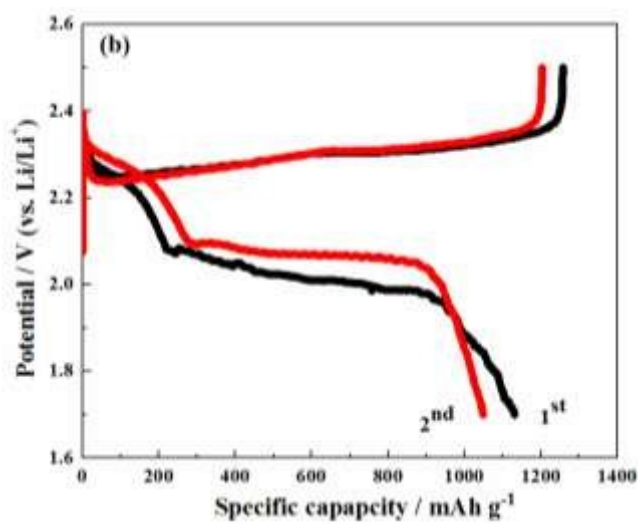


Fig.8b

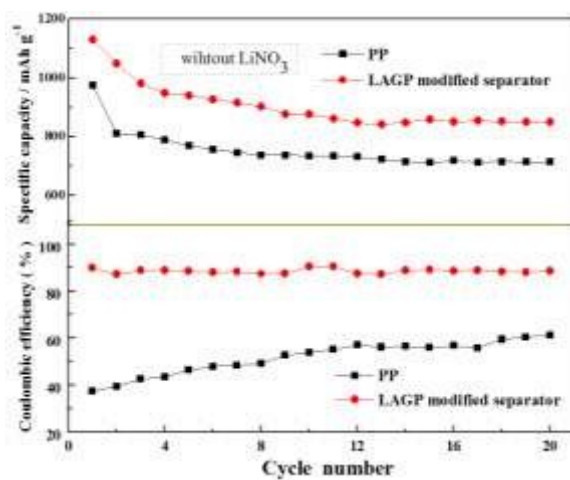


Fig.9

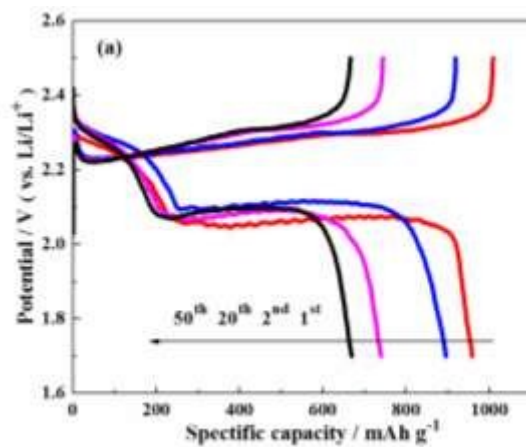


Fig.10a

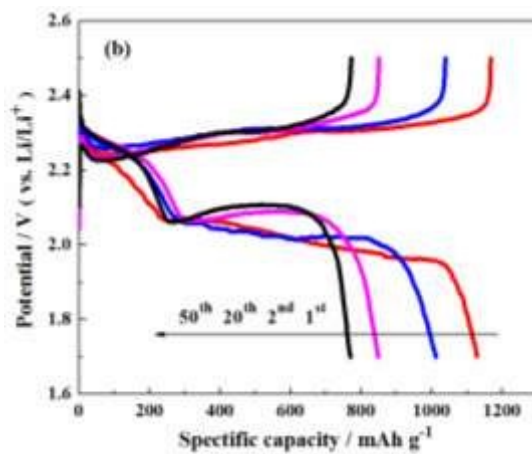


Fig.10b

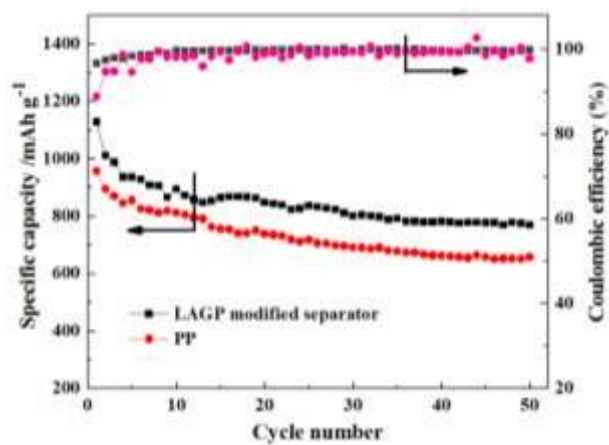


Fig. 11

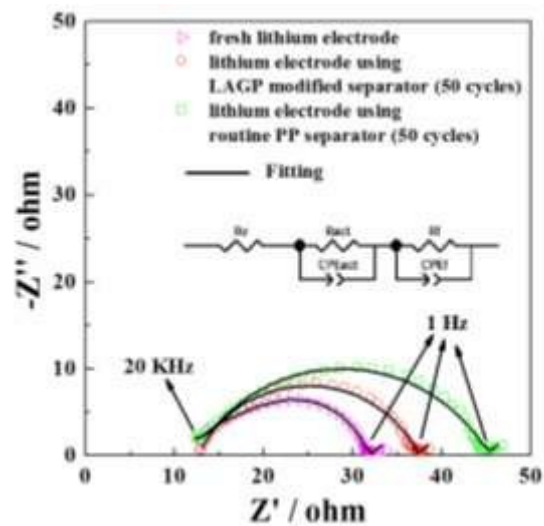


Fig.12

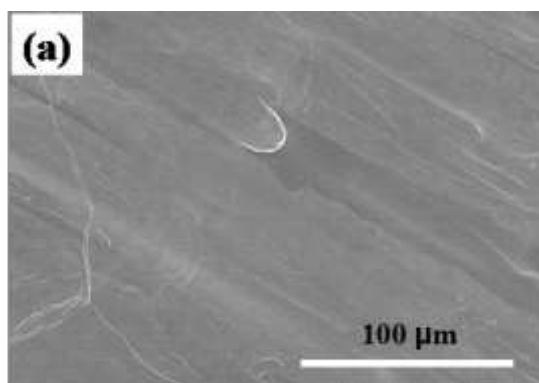


Fig.13a

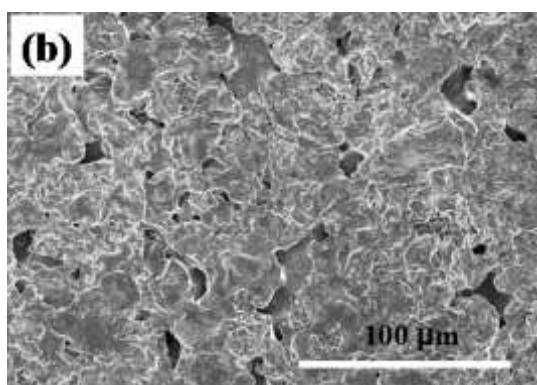


Fig.13b

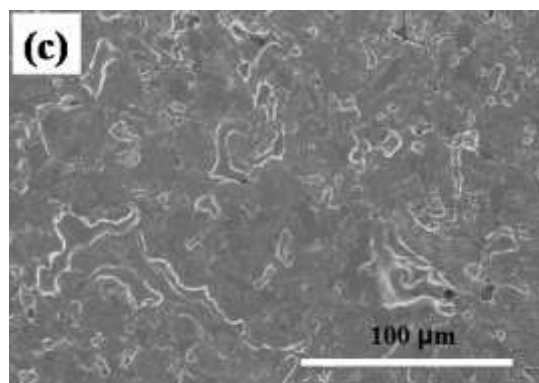


Fig.13c

Table 1 Comparison of the basic physical parameters of the PP, LAGP modified separator, LAGP glass ceramic plate

Separator code	Thickness (μm)	Contact angle ($^{\circ}$)	Gurley value ($\text{sec } 100 \text{ ml}^{-1}$)
PP	40	27.47	647.1
LAGP modified separator	51.6	20.48	2102.3
LAGP glass ceramic plate	600	37.15	—

Table 2 Fitted values of the impedance spectra in Fig.12

	R_e	R_{act}	R_f
Fresh Li	10.35	4.88	15.33
Li (50 cycles) with PP	10.54	4.63	28.31
Li (50 cycles) with LAGP modified separator	10.48	4.75	20.26

